Molecular Biology of the Cell
Vol. 12, 2601–2613, September 2001

Dad1p, Third Component of the Duo1p/Dam1p Complex Involved in Kinetochore Function and Mitotic Spindle Integrity

Maria Enquist-Newman,*† Iain M. Cheeseman,*† David Van Goor,‡ David G. Drubin,* Pamela B. Meluh,‡ and Georjana Barnes*§

*Department of Molecular and Cell Biology, University of California, Berkeley, California 94720-3202; and ‡Memorial Sloan-Kettering Cancer Center, New York, New York 10021

Submitted February 28, 2001; Revised June 19, 2001; Accepted June 29, 2001
Monitoring Editor: Douglas Koshland

We showed recently that a complex between Duo1p and Dam1p is required for both spindle integrity and kinetochore function in the budding yeast *Saccharomyces cerevisiae*. To extend our understanding of the functions and interactions of the Duo1p/Dam1p complex, we analyzed the novel gene product Dad1p (for Duo1 and Dam1 interacting). Dad1p physically associates with Duo1p by two-hybrid analysis, coimmunoprecipitates with Duo1p and Dam1p out of yeast protein extracts, and shows interdependent localization with Duo1p and Dam1p to the mitotic spindle. These results indicate that Dad1p functions as a component of the Duo1p/Dam1p complex. Like Duo1p and Dam1p, Dad1p also localizes to kinetochore regions in chromosomes spreads. Here, we also demonstrate by chromatin immunoprecipitation that Duo1p, Dam1p, and Dad1p associate specifically with centromeric DNA in a manner that is dependent upon Ndc10 and partially dependent upon the presence of microtubules. To explore the functions of Dad1p in vivo, we generated a temperature-sensitive allele, *dad1-1*. This allele shows spindle defects and a mitotic arrest phenotype that is dependent upon the spindle assembly checkpoint. In addition, *dad1-1* mutants undergo chromosome mis-segregation at the restrictive temperature, resulting in a dramatic decrease in viability.

INTRODUCTION

The spindle in *Saccharomyces cerevisiae* functions to segregate chromosomes faithfully during mitosis. For this complex process to occur, the mitotic spindle must undergo a number of changes over the course of the cell cycle (reviewed in Winey and O'Toole, 2001). In budding yeast, the nuclear envelope never breaks down and nuclear microtubules are present throughout the cell cycle, resulting in a spindle cycle that differs slightly from that of vertebrate cells. First, the spindle pole body duplicates after passage through G_1. A bipolar spindle then assembles during S phase and establishes attachments to paired sister chromatids. After the transition to anaphase and the loss of sister chromatid cohesion, chromatids separate and spindle elongation occurs to segregate the chromosomes. Finally, the spindle breaks down as the cells exit mitosis.

Unlike the spindles found in vertebrates, the budding yeast spindle contains a single microtubule attached to each chromosome and an average of five interpolar microtubules (Winey *et al.*, 1995). Therefore, faithful chromosome segregation requires that all chromosome–microtubule and intermicrotubule connections function correctly. The attachment between a chromosome and a microtubule occurs at kinetochores, the proteinaceous structure that assembles on centromeric DNA. Although many components of the yeast kinetochore have been characterized, particularly those that bind directly to DNA (reviewed in Pidoux and Allshire, 2000), complete elucidation of kinetochore activities requires the identification of all of the proteins involved. In particular, the mechanism by which the kinetochore attaches to a spindle microtubule, and how this attachment is regulated, are still unclear. A microtubule binding activity has previously been associated with kinetochores assembled on centromeric DNA in yeast extracts (Kingsbury and Koshland, 1993; Sorger *et al.*, 1994; Severin *et al.*, 1997); however, the proteins required for this activity remain elusive.

† These authors contributed equally to this work.
§ Corresponding author. E-mail address: gbarnes@socrates.berkeley.edu.

Abbreviations used: BLAST, basic local alignment search tool; ChIP, chromatin immunoprecipitation; DAPI, 4′,6-diamidino-2-phenylindole; GFP, green fluorescent protein; HA, influenza virus hemagglutinin epitope.

In addition to proteins that function to generate the attachments between chromosomes and microtubules, a number of microtubule-associated proteins are required to facilitate bipolar spindle assembly and integrity, and to provide the forces required for spindle elongation and chromosome segregation (reviewed in Winsor and Schiebel, 1997). In yeast, these proteins include kinesin-related motors such as Cin8p, Kip1p, Kip3, and Kar3p (Roof *et al*., 1992; Saunders and Hoyt, 1992; Saunders *et al*., 1997; Straight *et al*., 1998), which provide spindle forces and structure. There are also nonmotor microtubule-associated proteins such as *Stu*1p (Pasqualone and Huffaker, 1994) and Ase1p (Pellman *et al*., 1995) that play structural roles, such as Ase1p's role in cross-linking microtubules at the spindle midzone.

DNA microarray analysis has revealed that many of the genes required for spindle function in yeast are transcriptionally regulated, peaking in late G_1 or early S phase (Spellman *et al*., 1998). Recent genome-wide yeast two-hybrid screens (Ito *et al*., 2000; Uetz *et al*., 2000) have also helped identify protein–protein interactions that might occur within the spindle. Here we have used this combination of genomic resources to implicate a previously uncharacterized gene product, Dad1p, as a component of the Duo1p/Dam1p complex. A protein complex consisting of Duo1p and Dam1p has been previously shown to be required for the function of both the mitotic spindle and the kinetochore in budding yeast (Hofmann *et al*., 1998; Jones *et al*., 1999; Cheeseman *et al*., 2001). Interestingly, in addition to associating with kinetochores, Dam1p binds to microtubules directly in vitro (Hofmann *et al*., 1998), suggesting that this complex may play a role in generating kinetochore–microtubule connections. In this study, we provide evidence that Dad1p (for Duo1 and Dam1 interacting) is a novel subunit of the Duo1p/Dam1p complex. Dad1p localizes to the mitotic spindle and kinetochores, associates with Duo1p and Dam1p in vivo, and *dad1* mutants show phenotypes that indicate a role in spindle integrity and kinetochore function.

MATERIALS AND METHODS

Strains and Growth Conditions

The yeast strains used in this study are listed in Table 1. Yeast media were prepared as described previously (Rose *et al*., 1990). SM (synthetic medium) with appropriate nutrients, and YP (yeast extract/peptone) were supplemented with 2% glucose or with 2% raffinose and 2% galactose. Unless otherwise stated, yeast strains were grown in YPD (YP + dextrose). Benomyl was used at 20 μg/ml, a concentration at which wild-type yeast strains grew albeit with a reduced rate of growth. Geneticin (G418; Invitrogen, Carlsbad, CA) was used at 0.4 mg/ml. For temperature-shift experiments, overnight cultures were diluted to early log phase, grown for 2 h at 25°C, and then shifted to 37°C. Cell viability was measured by plating cells at the permissive temperature (25°C) and comparing the number of colonies formed to the total number of cells plated. The number of cells plated was determined by counting cells in a known volume with the use of a hemacytometer (Fisher Scientific, Pittsburgh, PA). Alpha factor arrest experiments were conducted by incubating log phase cells in fresh YPD containing 15–20 μg/ml alpha factor. To determine the percentage of large budded cells, cells with a bud greater than half the size of the mother cell were scored as large budded. Before counting, cells were fixed in formaldehyde and sonicated briefly. Three hundred cells were counted for each time point unless otherwise stated. The strains used for the LacI-green fluorescent protein (GFP) experiments were grown in YPD supplemented with 250 μM $CuSO_4$ (Fisher Scientific) to induce expression of the LacI-GFP fusion protein and with 0.02% adenine to reduce background fluorescence.

Sequence Analysis

Homologs of Dad1p were identified with the use of the BLAST program at http://www.blast.genome.ad.jp and http://www.ncbi.nlm.nih.gov/blast, as well as BLAST searches of organism-specific databases (*Aspergillus nidulans* at http://www.genome.ou.edu/fungal.html and *Candida albicans* at http://candida.stanford.edu). Sequences were aligned with the use of ClustalW (http://www2.ebi.ac.uk/clustalw). Alignments were formatted with the use of SeqVu 1.0.1 software (The Garvan Institute of Medical Research, Sydney, Australia). Homologous residues were assigned in this program with the use of the Karlin-Brendel setting. All other programs were run with the use of default settings.

Deletion and C-Terminal Epitope Tagging of DAD1

A complete deletion of the *DAD1* open reading frame was created by a one-step gene replacement with *HIS3* in DDY1102 to generate DDY2124. A polymerase chain reaction (PCR) product with 50 bp of the *DAD1* flanking regions on either side of *HIS3* was amplified from pRS303 with the use of primers oME2 (GTA GGA ATA GGA CTG ATG AAG AGC TCG GAC GTG TGA GGA TAT ATG TAC ATC AGA TTG TAC TGA GAG TGC ACC) and oME6 (GTA AAC ATA AAT TTA GGA TAA TAT TAG GAG AGA CAG AGG GAA CCG CAA CTC TGT GCG GTA TTT CAC ACC GC) and transformed into DDY1102. His^+ transformants were selected and correct integration was confirmed by PCR. This hemizygous strain (DDY2124) was subsequently sporulated and dissected onto YPD. C-Terminal GFP, influenza virus hemagglutinin epitope (HA), and myc epitope tags for *DAD1* were amplified from the templates pFA6a-GFP(S65T)-HIS3MX6 (GFP tag and the *HIS3* gene), pFA6a-3HA-His3MX6 (HA tag and the *HIS3* gene), and pFA6a-13MYC-His3MX6 (myc tag and *HIS3* gene) with the use of the primers oME16 (GAC GAA GCG CCC ATC GAC GAG CAA CCT ACT TTA TCT CAA TCG AAA ACG AAG CGG ATC CCC GGG TTA ATT AA) and oME17 (GTA AAC ATA AAT TTA GGA TAA TAT TAG GAG AGA CAG AGG GAA CCG CAA CTG AAT TCG AGC TCG TTT AAA C) as described (Longtine *et al*., 1998). The PCR products were subsequently transformed into the wild-type haploid strain DDY904. His^+ strains were selected and correct integration was confirmed by PCR.

Overexpression Plasmids

A *DAD1* overexpression plasmid was constructed by amplifying the *DAD1* open reading frame by PCR from wild-type genomic DNA with the use of primers oCH65 (GCG GGA TCC ATG ATG GCT AGT ACA TCC AAT G) and oCH66 (GCT CTA GAC AAC TAA GTT CAA AGA GG). The resulting DNA fragment was subsequently cloned behind the GAL1 promoter in pDD424, generating pDD1001. A plasmid to co-overexpress *DUO1* and *DAM1* was constructed by cloning the *DUO1* and *DAM1* open reading frames into the *Not*I/*Sac*I and *Bam*HI/*Nhe*I sites of pESC-LEU (Stratagene, La Jolla, CA), respectively, to generate pIC68.

Immunofluorescence Microscopy

Indirect immunofluorescence microscopy was performed as described (Ayscough and Drubin, 1998) with the use of antibodies at the following dilutions: 1:200 for the YOL134 anti-tubulin antibody (rat; Accurate Chemical & Scientific, Westbury, NY), 1:4000 for the anti-GFP antibody (rabbit; a generous gift from Pam Silver, Dana-Farber/Harvard Medical School, Cambridge, MA), 1:1000 for the anti-HA antibody (mouse; Covance, Princeton, NJ), 1:2000 for the affinity-purified rabbit anti-Duo1p antibody (Hofmann *et al*., 1998), and 1:1000 for the affinity-purified guinea pig anti-Dam1p antibody

Table 1. Yeast strains used in this study

Name	Genotype	Source
DDY1102	*MAT***a**/*MAT*α, *his3*Δ*200/his3*Δ*200, leu2-3,112/leu2-3,112 ura3-52/ura3-52, ade2-1/ADE2, lys2-801/LYS2*	1
DDY2124	*MAT***a**/*MAT*α, *his3*Δ*200/his3*Δ*200, leu2-3,112/leu2-3,112, ura3-52/ura3-52, ade2-1/ADE2, lys2-801/LYS2, dad1*Δ*::HIS3/DAD1*	2
DDY902	*MAT***a**, *his3*Δ*200, leu2-3,112, ura3-52, ade2-1*	1
DDY904	*MAT*α, *his3*Δ*200, leu2-3,112, ura3-52, lys2-801*	1
DDY2125	*MAT***a**, *his3*Δ*200, leu2-3,112, ura3-52, lys2-801, dad1*Δ*::HIS3, pDD1002 (DAD1, CEN, URA3)*	2
DDY2126	*MAT***a**, *his3*Δ*200, leu2-3,112 ura3-52, ade2-1, dad1-1::KanMX*	2
DDY2127	*MAT*α, *his3*Δ*200, leu2-3,112, ura3-52, lys2-801, dad1-1::KanMX*	2
DDY2128	*MAT***a**, *his3*Δ*200, leu2-3,112, ura3-52, ade2-1, dad1-1::LEU2*	2
DDY2129	*MAT*α, *his3*Δ*200, leu2-3,112, ura3-52, lys2-801, dad1-1::LEU2*	2
DDY2130	*MAT*α, *his3*Δ*200, leu2-3,112, ura3-52, lys2-801, DAD1-GFP::HIS3*	2
DDY2131	*MAT*α, *his3*Δ*200, leu2-3,112, ura3-52, lys2-801, DAD1-3xHA::HIS3*	2
DDY2166	*MAT***a**, *his3*Δ*200, leu2-3,112, ura3-52, ade2-1, DAD1-13xMYC::HIS3*	2
DDY2132	*MAT***a**, *his3*Δ*200, leu2-3,112, ura3-52, ade2-1, DAD1-GFP::HIS3, duo1-2::LEU2*	2
DDY2133	*MAT***a**, *his3*Δ*200, leu2-3,112, ura3-52, lys2-801, DAD1-GFP::HIS3, dam1-11:KanMX*	2
DDY1788	*MAT***a**, *his3*Δ*200, leu2-3,112, ura3-52, ade2-1, mad2*Δ*::URA3*	2
DDY2134	*MAT***a**, *his3*Δ*200, leu2-3,112, ura3-52, dad1-1::LEU2, mad2*Δ*::URA3*	1
DDY2135	*MAT***a**, *his3*Δ*200, leu2-3,112, ura3-52, dad1-1::KanMX, duo1-1::LEU2*	2
DDY1921	*MAT***a**, *his7, ura1, cdc15-1*	1
DDY2136	*MAT***a**, *dad1-1::KanMX, mad2*Δ*::URA3, cdc15-1*	2
DDY1925	*MAT***a**, *his3*Δ*200, ura3-52, ade2-1, HIS3::pCu-LacI-GFP, leu2-3,112::lacO::LEU2*	1
DDY2137	*MAT***a**, *his3*Δ*200, ura3-52, ade2-1, HIS3::pCu-LacI-GFP, leu2-3,112::lacO::LEU2, dad1-1::KanMX, mad2*Δ*::URA3*	2
DDY2138	*MAT***a**, *his3*Δ*200; leu2-3,112, ura3-52, lys2-801, NDC10-GFP::HIS3, DAD1-3xHA::HIS3*	2
DDY1484	*MAT*α, *lys2-801, ade2-101, his3*Δ*200, leu2-*Δ*1, ura3-52, TUB1::LYS2, bim1*Δ*::URA3*	4
DDY1514	*MAT***a**, *his3*Δ*200, leu2-3,112, ura3-52, lys2-801, trp1*Δ*1, mps1-1*	3
DDY1529	*MAT***a**, *his3*Δ*200, leu2-3,112, ura3-52, stu1-5*	5
DDY1806	*MAT***a**, *his3*Δ*200, leu2-3,112, ura3-52, ade2-101, cin8*Δ*::URA3*	6
DDY1504	*MAT***a**, *his3*Δ*200, leu2-3,112, ura3-52, lys2-801, bub1*Δ*::HIS3*	6
DDY1505	*MAT***a**, *his3*Δ*200, leu2-3,112, ura3-52, ade2-101, lys2-801, bub3*Δ*::LEU2*	6
DDY2088	*MAT*α, *his3*Δ*200, leu2-3,112, ura3-52, lys2-801, trp1-1, bir1-*Δ*11::LEU2*	7
DDY1943	*MT***a**, *his3*Δ*200, leu2*Δ*1, ura3-52, ade2-101, lys2-801, trp1*Δ*1, ctf19*Δ*::HIS3*	8
MS10	*MAT***a**, *ura3-52, leu2-3,112, ade2-101* (S288C)	
PM1021-20A	*MAT***a**, *ura3-52, ade2-101, trp1-*Δ*1, lys2-801, ndc10-42*	9
YPH499	*MAT***a**, *ura3-52, leu2-*Δ*1, ade2-101, trp1-*Δ*63, his3-*Δ*200, lys2-801*	8

Sources: 1, Drubin lab; 2, this study; 3, Mark Winey; 4, David Botstein; 5, Tim Huffaker; 6, M. Andy Hoyt; 7, Clarence Chan; 8, Phil Heiter; 9, Meluh lab.

All Drubin lab strains are derived from strain S288C.

(Cheeseman *et al.*, 2001). Fluorescein and rhodamine-conjugated anti-IgG heavy chain secondary antibodies (Jackson Laboratories, West Grove, PA) were used at a dilution of 1:100 and a Cy3-conjugated goat anti-rabbit secondary antibody (Sigma, St. Louis, MO) was used at a dilution of 1:2000. Microscopy was performed with the use of a Nikon TE300 microscope (Melville, NY) equipped with a 100× Plan-Apo/1.4 N.A. objective and 1.4 N.A. condenser. Images were acquired with a Orca 100 charge-coupled device camera (Hamamatsu, Bridgewater, NJ) and Phase 3 Imaging software (Phase 3 Imaging, Glen Mills, PA).

Generation of dad1-1 Temperature-sensitive Mutant

To construct a *DAD1* template for mutagenesis, *S. cerevisiae DAD1* was amplified from genomic DNA by PCR with the use of primers oME18 (GCG CGG GAT CCG TAA ATG CAT TTA TCT AT) and oME19 (GCG CGT CTA GAT TCT AAC AAG GTT AAA TAT). This fragment was cloned into pRS316 and pRS315, making pDD1002 and pDD1003, respectively. DDY2124 (diploid heterozygous for *dad1*Δ*::HIS3*) was transformed with pDD1002, sporulated, and dissected. His^+, Ura^+ haploids were selected (DDY2125). pDD1003 was mutagenized in vitro with the use of hydroxylamine (Sigma) as described previously (Hofmann *et al.*, 1998). The mutagenized plasmids were transformed into DDY2125. These transformants (8000 total) were then plated onto 5-fluoroorotic acid to select against the original, wild-type plasmid. Strains that grew at 25°C but not at 37°C were identified. Plasmids from these strains were rescued and retransformed into DDY2125 to confirm the heat sensitivity.

The *dad1-1* allele was subsequently integrated into the genome. The *Not*I site in the polylinker of pDD1003 was made blunt with Klenow and then *DAD1* was mutagenized with the use of the Transformer Site-Directed Mutagenesis kit (CLONTECH, Palo Alto, CA) with mutagenesis oligo oME20 (CCT AAT GAT AAG TAA GTT GCG GCC GCC TTT TGC ACG TTG AAA AAA G) to introduce a new *Not*I site 120 bp downstream from the *DAD1* open reading frame. The KanMX gene from pUG6 was cloned into the *Not*I site in the same orientation as *DAD1* to create pDD1004. The *LEU2* gene from pKK582 was cloned into the *Not*I site in the opposite orientation from *DAD1* to create pDD1005. *dad1-1* was swapped into these plasmids with the use of the SmaBI and the *Nde*I sites, creating pDD1006 and pDD1007. pDD1006 and pDD1007 were then digested with the use of *Bam*HI and *Sac*II or *Bam*HI and *Xba*I sites, respectively. The fragment containing *dad1-1* was then transformed

into DDY2124. G418$^+$, His$^-$ (and Leu$^+$, His$^-$) diploids were selected and the integration was confirmed by PCR. Diploids were sporulated and haploid integrants were recovered (Table 1).

Immunoprecipitation and Immunoblot Procedures

Immunoprecipitation was performed as described in Cheeseman *et al.* (2001). Briefly, 50 ml of yeast cultures at OD_{600} = 1.2 were spun down and washed with sorbitol buffer (1.3 M sorbitol, 0.1 M potassium phosphate pH 7.5). Cells were then incubated with lyticase for 30 min at 30°C, pelleted gently, and resuspended in lysis buffer (50 mM Tris-HCl pH 8.0, 150 mM NaCl, 1% NP-40) with protease inhibitors and 1 mM phenylmethylsulfonyl fluoride. The lysate was then sonicated three times for 15 s and then pelleted for 15 min in a microcentrifuge. Anti-Duo1p antibody (6 μl) (Hofmann *et al.*, 1998), 6 μl of anti-Dam1p antibody (Cheeseman *et al.*, 2001), 4 μl of anti-HA antibody (HA.11; Covance), and 6 μl of preimmune antibody were prebound to 12 μl of protein A Affi-gel beads (Bio-Rad, Hercules, CA). Extract from the equivalent of 15 OD_{600} units of yeast was added to each aliquot of the precoupled protein A Affi-gel beads and samples were incubated overnight at 4°C. Samples were then washed three times with lysis buffer and sample buffer was added.

Immunoblot analysis was performed with the use of standard SDS-PAGE and immunoblot transfer methods. Anti-GFP antibody (rabbit; from Pam Silver) was used at a dilution of 1:10,000, anti-HA antibody (Covance) was used at a dilution of 1:1000, anti-Duo1p antibody (Hofmann *et al.*, 1998) was used at a dilution of 1:2000, and anti-Dam1p antibody (Cheeseman *et al.*, 2001) was used at a dilution of 1:1000. Anti-rabbit and anti-mouse horseradish peroxidase-conjugated secondary antibodies (Amersham Pharmacia Biotech, Piscataway, NJ) were used at a dilution of 1:10000, and anti-guinea pig horseradish peroxidase-conjugated secondary antibody (Alpha Innotech, San Leandro, CA) was used at a dilution of 1:9000.

Chromatin Immunoprecipitations

Immunoprecipitation of formaldehyde cross-linked chromatin was performed essentially as described (Meluh and Koshland, 1997), with the following changes. After fixation in 1% formaldehyde for 2 h, cells were harvested and washed three times with Tris-buffered saline (100 mM Tris pH 7.4, 150 mM NaCl), after which cell pellets were stored at −80°C. As required, cell pellets were thawed on ice, resuspended in SDS lysis buffer (1% SDS, 10 mM EDTA, 50 mM Tris pH 8.1) supplemented with protease inhibitors, and disrupted by glass bead mechanical breakage. Subsequent sonication, centrifugation, immunoprecipitation, and elution steps were as described previously (Meluh and Koshland, 1997), except that the 65°C incubation to reverse the formaldehyde cross-links was extended to overnight. For experiments involving the Dad1-13myc-tagged strain, an FA lysis buffer (50 mM HEPES/KOH pH 7.5, 140 mM NaCl, 1 mM EDTA, 1% [vol/vol]) Triton X-100, 0.1% [wt/vol] sodium deoxycholate) was used instead (Meluh and Broach, 1999).

Affinity-purified rabbit anti-Duo1p antibody was used at a 1:200 dilution (5 μl/ml). Affinity-purified guinea pig anti-Dam1p antibody was antibody was used at a 1:150 dilution (6.5 μl/ml). For the experiments in Figure 7B, an affinity-purified rabbit anti-Dam1p antibody was also used (Cheeseman, unpublished data) at a dilution of 1:150 (6.5 μl/ml). Purified anti-myc monoclonal antibody (Covance) was used at a dilution of 1:100 (10–10 μg/ml final concentration). Competitor Myc peptide (Covance) was added in 200–500-fold molar excess relative to anti-Myc. Crude anti-Mif2p rabbit antiserum (C223) was used at a dilution of 1:250 (4 μl/ml; Meluh and Koshland, 1997). Affinity-purified anti-Ndc10p antibody, generously provided by Kenneth Kaplan (University of California, Davis, CA), was used at a 1:100 dilution (10 μl/ml). Immunecomplexes were isolated on protein A Sepharose CL-4B beads (Amersham Pharmacia Biotech).

PCR reactions used *Taq* polymerase from Promega (Madison, WI) and were typically for 24 cycles. PCR products were resolved on 8% Tris borate-EDTA-PAGE and visualized with ethidium bromide. Stained PCR products were imaged with a Bio-Rad Chemi-Doc Mac Gel Documentation system and quantitated with the use of Quantity One image analysis software (Bio-Rad).

RESULTS

Identification of Dad1p

We recently showed that Duo1p and Dam1p form a protein complex that is required for both spindle integrity and kinetochore function in yeast (Cheeseman *et al.*, 2001). To increase our understanding of the functions of this complex, we developed a strategy to identify additional polypeptides that interact with Duo1p and Dam1p. The transcription of both *DUO1* and *DAM1* is cell cycle regulated, peaking in late G_1 or early S phase (Spellman *et al.*, 1998). Therefore, to determine whether any of the 13 gene products previously identified in a two-hybrid screen conducted with the use of Duo1p as a bait (Hofmann *et al.*, 1998) was likely to function with Duo1p and Dam1p, we conducted a search of the Yeast Cell Cycle Analysis Project database (http://genome-www.stanford.edu/cgi-bin/cellcycle/search; Spellman *et al.*, 1998) for genes that have an expression pattern similar to *DUO1* and *DAM1*. We found that, in addition to being a positive in the Duo1p two-hybrid screen (Hofmann *et al.*, 1998), YDR016c had a very similar transcription profile to *DAM1*. Recently, two genome-wide two-hybrid screens have confirmed the two-hybrid interaction between YDR016c and Duo1p (Ito *et al.*, 2000; Uetz *et al.*, 2000). Based on these data and on the analysis presented in this article, we named this gene *DAD1*, for Duo1 and Dam1 interacting. Dad1p consists of 94 amino acids with a predicted molecular mass of 10.5 kDa.

To determine whether *DAD1* is an essential gene in *S. cerevisiae*, we constructed a deletion of the entire *DAD1* open reading frame by replacing it with the *HIS3* gene (see MATERIALS AND METHODS), creating a hemizygous null diploid strain. When the resulting strain was sporulated and dissected it gave rise to a 2:2 segregation of viable to dead spores with no His$^+$ strains recovered, indicating that *DAD1* is an essential gene. When the inviable spores were examined under a dissecting microscope, it was found that they had germinated and given rise to two or three large budded cells (our unpublished results).

Homologs of Duo1p and Dam1p exist in a variety of fungal species (Cheeseman *et al.*, 2001). If Dad1p functions in the Duo1p/Dam1p complex then it might also be conserved. BLAST searches were conducted with the use of the entire Dad1p protein as the query sequence. Although no definitive metazoan homologs were identified, homologs with >24% identity were found in four different fungal species, with many of residues being conserved in several proteins (Figure 1). In addition, the Dad1p homologs are similar in size, and high homology is distributed throughout the entire lengths of these proteins. We conclude that they are likely to be true Dad1p homologs.

DUO1 and *DAM1* cause lethality when overexpressed either alone or in combination (Hofmann *et al.*, 1998; our unpublished results). In contrast, overexpression of *DAD1* from a galactose-inducible *GAL1* promoter had no effect on

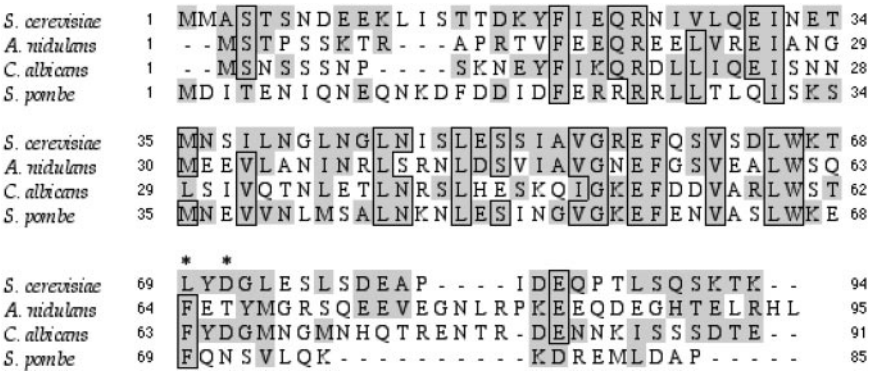

Figure 1. Dad1p has homologs in other fungal species. Residues identical in at least three of the four proteins are boxed and conserved residues are highlighted. Residues mutated in *dad1-1* are indicated with an asterisk. In pairwise alignments, *S. cerevisia*e Dad1p is 29% identical (27 of 94) and 49% conserved (46 of 94) with the *A. nidulans* homolog (from 13d09a1.r1), 24% identical (22 of 91) and 46% conserved (42 of 91) with the *C. albicans* homolog (from sequencing of Contig6-2505), and 28% identical (24 of 85) and 52% conserved (44 of 85) with the *S. pombe* homolog (SPAC16A10.05C). Not shown is a homolog in a closely related *Saccharomycetales* species, which is 50% identical (47 of 94) and 68% conserved (64 of 94) with *S. cerevisiae* Dad1p.

either growth rate or spindle morphology, but was able to complement a deletion of *DAD1* (our unpublished results). Strikingly, *DAD1* overexpression was able to partially suppress the lethality, which results from *DUO1* and *DAM1* cooverexpression (our unpublished results). Because Duo1p and Dam1p function as a complex (Cheeseman *et al.*, 2001), the lethality that results from the overexpression of *DUO1* and *DAM1* may occur due to imbalances in the levels of these subunits. Therefore, the ability of *DAD1* to suppress this lethality may reflect an in vivo interaction and the restoration of proper subunit ratios for a ternary complex.

Dad1p Localizes to the Mitotic Spindle in a Duo1p- and Dam1p-dependent Manner

Duo1p and Dam1p localize to the mitotic spindle (Hofmann *et al.*, 1998; Jones *et al.*, 1999; Cheeseman *et al.*, 2001). To determine whether Dad1p shares a similar localization, we integrated a C-terminal GFP tag at the endogenous *DAD1* locus. This Dad1p-GFP fusion protein was fully functional because it showed no growth or spindle morphology defects (our unpublished results). The Dad1-GFP fusion protein was found to localize to what appeared to be mitotic spindles in live cells. When these cells were fixed and stained with antibodies against GFP and tubulin, it was found that Dad1-GFP did indeed colocalize with nuclear microtubules (Figure 2A). In G1 cells, Dad1-GFP colocalized with spindle poles, and in mitotic cells Dad1-GFP localized along the entire length of both short and long spindles. Dad1-GFP was not detected on cytoplasmic microtubules.

To test whether Dad1p localization was dependent upon Duo1p and Dam1p function, strains with different *duo1* and *dam1* alleles in combination with Dad1-GFP fusion protein were constructed. In *duo1-2* and *dam1-1* mutant cells, Dad1-GFP was still properly localized to both short and long mitotic spindles even after 1.5 h at 37°C (Figure 2B; our unpublished results). However, these cells did show a somewhat weaker Dad1-GFP signal, especially in the middle of the spindle. In contrast, Dad1-GFP is delocalized in a temperature degron-tagged allele of *duo1* (*duo1*^{td}), *dam1-9*, *dam1-11*, and *dam1-19* mutants. At the permissive temperature (25°C), some Dad1-GFP delocalization was observed in these mutants compared with wild-type cells. However, after incubation at the restrictive temperature, no localization was detected by immunofluorescence (Figure 2B; our unpublished results). Even although Dad1p appears delocalized in these cells, the protein level of the Dad1-GFP fusion in these mutants was indistinguishable from wild type (our unpublished results). Duo1p and Dam1p were also found to be delocalized in *dad1-1* mutants at both the permissive and nonpermissive temperature (our unpublished results), similar to what has been described previously for *duo1* and *dam1* mutants (Cheeseman *et al.*, 2001). These data show that Duo1p, Dam1p, and Dad1p are mutually dependent for localization to the mitotic spindle.

Dad1p Physically Associates with Duo1p and Dam1p

To test whether Dad1p physically associates with Duo1p and Dam1p in vivo, coimmunoprecipitations were performed with the use of a Dad1p-HA-tagged strain. When an anti-HA antibody was used, Dad1p-HA, Duo1p, and Dam1p were immunoprecipitated from yeast protein extracts (Figure 3). Similarly, anti-Duo1p or anti-Dam1p antibodies immunoprecipitated Dad1p-HA, Duo1p, and Dam1p. These interactions were specific because none of these three proteins was precipitated with preimmune antibodies, or when the anti-HA antibody was used on extracts from a strain that did not express HA-tagged Dad1p (Figure 3). In addition, tubulin was not immunoprecipitated by any of these antibodies (our unpublished results). These data show that Dad1p physically associates with Duo1p and Dam1p in yeast protein extracts.

Generation of Temperature-sensitive dad1 Mutants

To determine the *DAD1* loss of function phenotype, we generated a temperature-conditional allele. *dad1-1* results from two point mutations: L69R and D71N. This allele is supersensitive to the microtubule-destabilizing drug benomyl and is heat sensitive at 37°C. When asynchronous *dad1-1* cultures were shifted to 37°C, the cells arrested with large buds and short mitotic spindles (Figure 4, A and B). This phenotype was observed in 60–70% of the cells 3 h after the shift to 37°C (Figure 4A). As with *duo1-2* and *dam1-9* mutants (Hofmann *et al.*, 1998; Cheeseman *et al.*, 2001), the cells eventually break through the arrest. Upon elimination of the spindle assembly checkpoint by deletion of *MAD2*, *dad1-1* mutants no longer arrest with large buds and are able to undergo spindle elongation when shifted to 37°C (Figure 4, A and B), indicating that the arrest is mediated by this

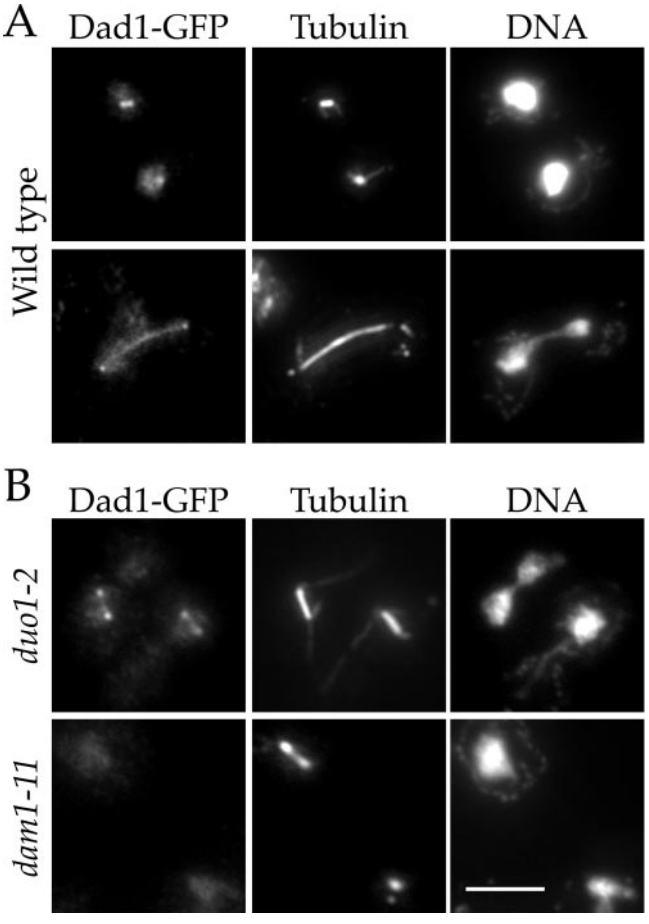

Figure 2. Dad1p localizes to the mitotic spindle in a Duo1p- and Dam1p-dependent manner. (A) Dad1-GFP localization in wild-type cells. Cells were grown to log phase and processed for immunofluorescence staining of Dad1-GFP (anti-GFP antibodies) and tubulin (anti-tubulin antibody), and for DNA (4′,6-diamidino-2-phenylindole [DAPI]). (B) Dad1-GFP localization in *duo1* and *dam1* mutants. Cells were grown at 25°C, shifted to 37°C for 1.5 h, and processed for immunofluorescence as described above. Bar, 5 μm.

checkpoint. *dad1-1 duo1-1* double mutants also arrest with large buds, but show a spindle phenotype similar to some *dam1* alleles in which the spindle has elongated prematurely and started to break down in the middle (Figure 4C; Cheeseman *et al*., 2001). *dad1-1* single mutants also show this phenotype after extended periods (4.5 h) at the nonpermissive temperature (Figure 4C).

Because *dad1-1* activates the spindle assembly checkpoint, the short spindle arrest is representative of the spindle phenotype during metaphase. To examine the spindle phenotype at later time points during mitosis, we arrested *dad1-1* mutants in telophase through the use of a temperature-sensitive *cdc15-1* allele in a strain also deleted for *MAD2* to allow passage through metaphase. When these strains were examined (Figure 4D), it was found that many spindles stained more faintly in the middle compared with wild type, suggesting that the spindle was broken down, while other mutant spindles appeared abnormally bent. The different spindle phenotypes observed during both metaphase and late mitosis demonstrate an important role for Dad1p in spindle integrity.

dad1-1 Shows Specific Genetic Interactions with a Subset of Mitotic Spindle Mutants

To gain further insights into the functions of Dad1p, we crossed *dad1-1* to mutants defective in spindle and kinetochore functions. *dad1-1* was synthetically lethal with *duo1-2*, as well as with a variety of *dam1* alleles (*dam1-1, dam1-9*, *dam1-11*, *dam1-19*), and showed synthetic sickness in combination with the weaker *duo1* allele, *duo1-1*, providing further evidence that Dad1p functions together with Duo1p and Dam1p. In addition, *dad1-1* was synthetically sick with mutants of the microtubule-associated proteins *Stu*1p (*stu1-5*) and Bim1p (*bim1*Δ). In the case of *bim1*Δ, only 20% of predicted *dad1-1 bim1*Δ double mutant spores were recovered and they were extremely slow growing. These interactions were specific because *dad1-1* did not show genetic interactions with deletions of the genes encoding the microtubule-associated proteins Ase1p, Bik1p, Cin8p, Dyn1p, or Kip3p. Kinetochore function also appears to be defective in *dad1-1* mutants because they showed synthetic lethality with a deletion of the gene encoding the kinetochore protein Bir1p. No genetic interactions were seen with other kinetochore mutants (*ndc10-1*, *ndc10-2*, and *ctf19*Δ). Mutants defective for spindle or kinetochore function often show synthetic defects with spindle assembly checkpoint mutants. In fact, we found that *dad1-1* was synthetically lethal with the spindle assembly checkpoint mutants *bub1*Δ and *bub3*Δ and was synthetically sick with *mps1-1*. In contrast, *dad1-1* did not show genetic interactions with *mad1*Δ, *mad2*Δ, *mad3*Δ, or *bub2*Δ. In total, these genetic interactions suggest that Dad1p has a function that is closely related to Duo1p and Dam1p, and plays a role in processes associated with both spindle and kinetochore function. Although genetic interactions were not observed with all spindle and kinetochore mutants tested, previous studies have indicated that such genetic

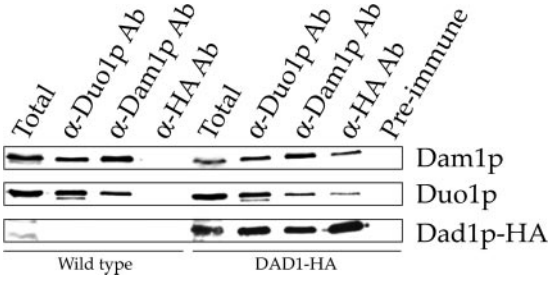

Figure 3. Dad1p associates with Duo1p and Dam1p in yeast protein extracts. Protein extracts from wild-type cells and protein extracts from a strain containing HA-tagged Dad1p were incubated with antibodies recognizing Duo1p, Dam1p, HA, or with preimmune serum bound to protein A beads (see MATERIALS AND METHODS). Immunoprecipitated samples were run on a 15% polyacrylamide gel and probed with antibodies recognizing either Duo1p, Dam1p, or HA. Duo1p, Dam1p, and Dad1-HA are specifically immunoprecipiated when antibodies against either Duo1p or Dam1p are used, but not with preimmune serum or in a strain that lacks the HA-tagged Dad1p.

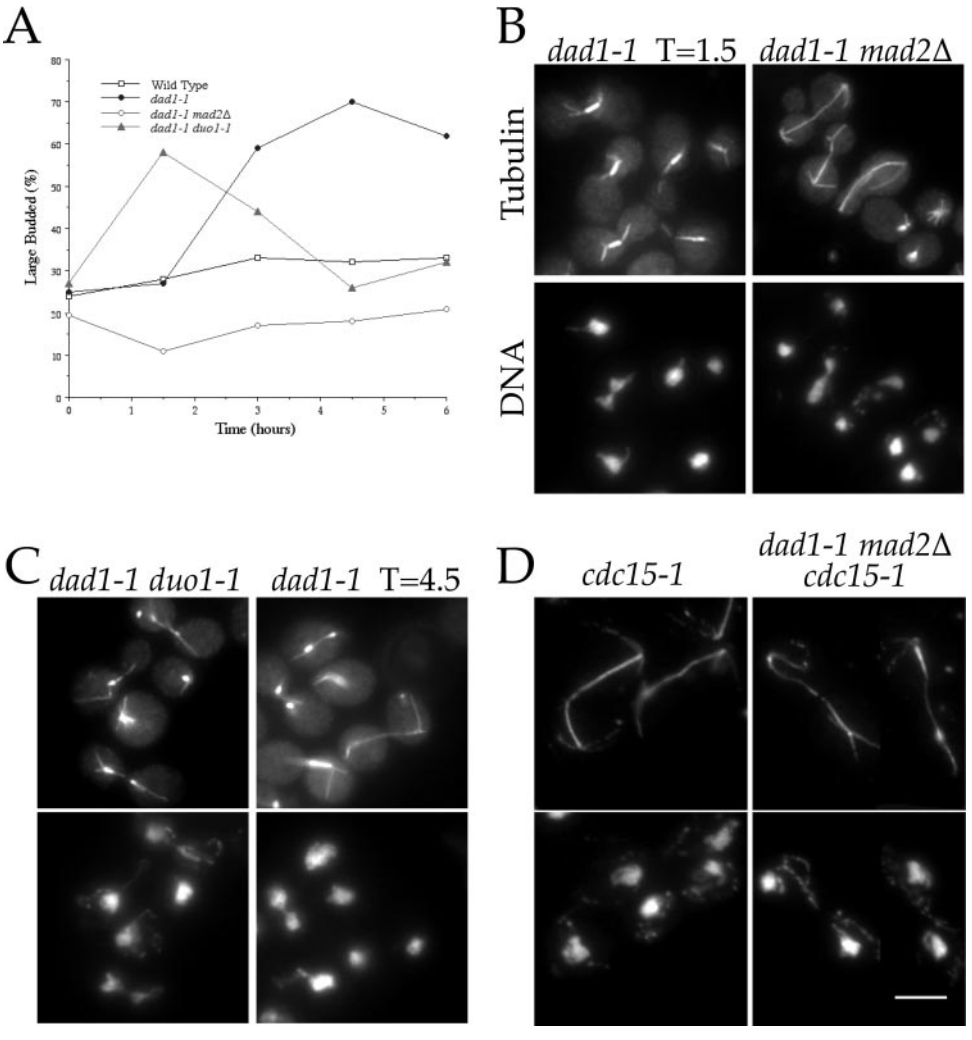

Figure 4. *dad1-1* shows mitotic defects. (A) Morphological arrest. Cells were grown to log phase at 25°C and shifted to 37°C at t = 0. The percentage of cells showing a large budded morphology was determined by counting a fixed and sonicated sample. (B) *dad1-1* mutant phenotype. Cells were grown at 25°C, shifted to 37°C for 1.5 h, and processed for tubulin immunofluorescence (anti-tubulin antibody) and DNA staining (DAPI). (C) Broken down spindle phenotypes in *dad1-1 duo1-1* double mutants or *dad1-1* mutants at later time points. Cells were grown at 25°C, shifted to 37°C for 1.5 h or 4.5 h as indicated, and processed for immunofluorescence as described above. (D) Late mitotic mutant phenotypes. Cells were arrested with alpha factor at 25°C, released to fresh prewarmed medium at 37°C for 3 h, and processed for immunofluorescence as described above. Bar, 5 μm.

interactions are likely to be allele-specific (Cheeseman *et al.*, 2001)

dad1-1 Undergoes Chromosome Mis-segregation at High Rates

duo1 and *dam1* mutants show a rapid drop in viability when they undergo mitosis (Jones *et al.*, 1999; Cheeseman *et al.*, 2001). We therefore chose to examine the kinetics of lethality in *dad1-1* mutants as they transit mitosis. At early time points, during which they were arrested with short spindles (t = 1.5 and 3 h), the viability of *dad1-1* mutants remained high (Figure 5A). However, at later time points, during which cells began to break through the arrest (t = 4.5 and 6 h), the viability dropped dramatically (Figure 5A). In contrast, a precipitous drop in viability was observed almost immediately in *dad1-1* cells that are prevented from arresting in response to spindle damage by deletion of *MAD2*. *dad1-1 duo1-1* double mutants also showed a dramatic drop in viability immediately after the shift to the nonpermissive temperature (37°C), indicating that the spindle assembly checkpoint is unable to prevent lethality in these cells.

To test whether the drop in viability might be due to an increase in chromosome mis-segregation, the fidelity in chromosome segregation was examined with the use of a LacI-GFP fusion protein to mark integrated LacO sequences (Belmont and Straight, 1998). Because *dad1-1* mutants arrest in metaphase before chromosome segregation, we monitored the fidelity of chromosome segregation in *dad1-1 mad2*Δ double mutants, which are able to progress through mitosis. For this experiment, a cell was scored as showing chromosome mis-segregation if two dots of LacI-GFP fluorescence were observed at one pole, or if only one dot of LacI-GFP fluorescence was observed, indicating two unresolvable sister chromatids at the same pole (Figure 5B). When 300 wild-type cells were scored, only one instance of chromosome mis-segregation was observed. Although no chromosome mis-segregation was observed in *dad1-1 mad2*Δ double mutant cells grown at the permissive temperature, 22% (n = 100) of large budded cells with two separate DNA masses showed chromosome mis-segregation after 1.5 h at the restrictive temperature, and 30% (n = 100) showed mis-segregation after 3 h (Figure 5B). These results are similar to

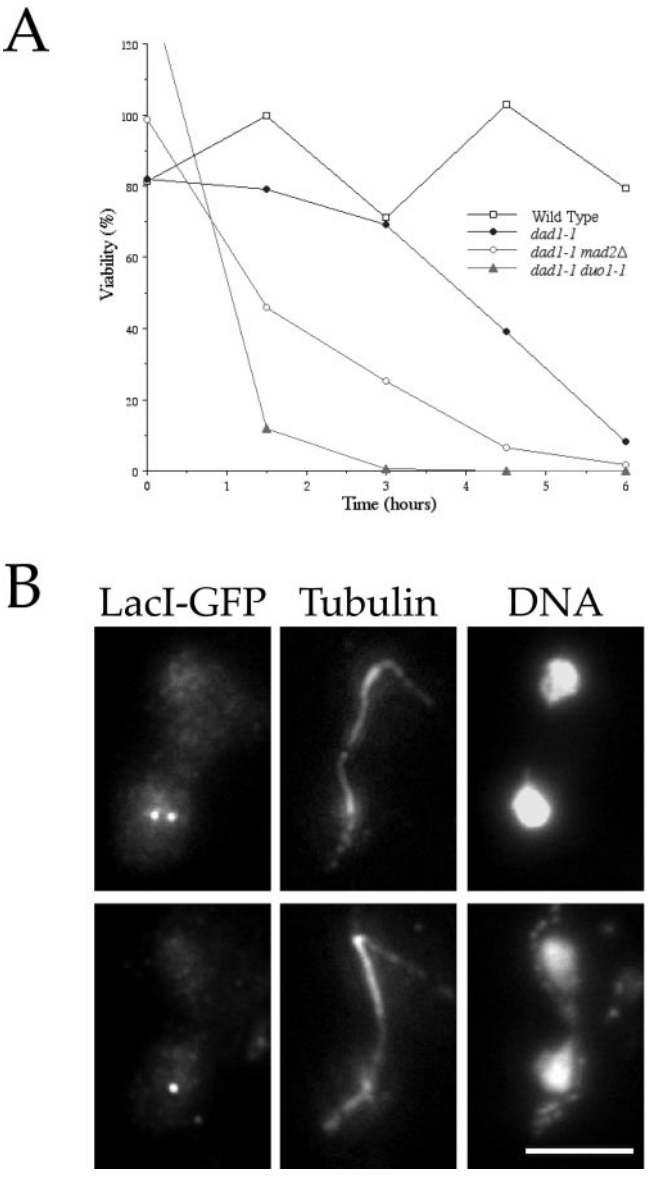

Figure 5. *dad1-1* mutants show chromosome segregation defects. (A) Viability of *dad1-1* mutants. Cells were grown to log phase at 25°C then shifted to 37°C at t = 0. For each time point, cells were plated onto plates containing YPD medium at 25°C and a sample was counted with the use of a hemacytometer to determine the cells per milliliter of culture. (B) Chromosome mis-segregation observed with the use of LacI-GFP system of chromosome tagging. *dad1-1 mad2*Δ double mutant cells were grown to log phase at 25°C, shifted to 37°C for 3 h, and processed for immunofluorescence staining for LacI-GFP (anti-GFP antibodies), tubulin (anti-tubulin antibody), and DNA (DAPI). Bar, 5 μm.

those obtained when the frequency of chromosome mis-segregation was determined in *duo1-2* and *dam1-9* mutants, which show a similar spindle phenotype to *dad1-1*, but are less dramatic than the 90% chromosome mis-segregation observed in *dam1-1* and *dam1-11* mutants (Cheeseman *et al.*, 2001).

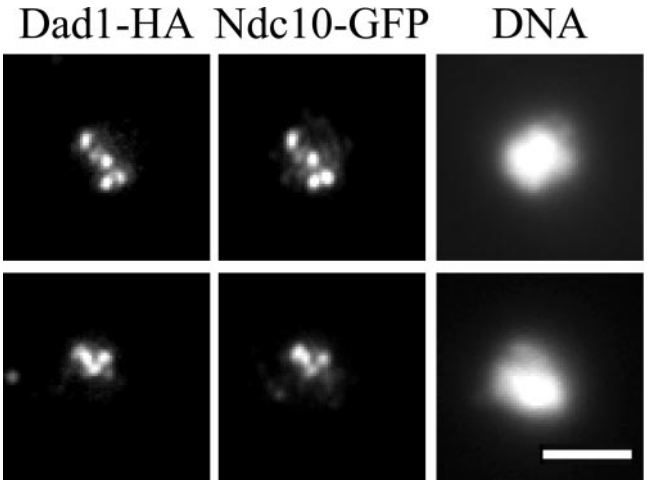

Figure 6. Dad1-HA localizes to kinetochores in spreads of mitotic chromosomes. Cells coexpressing Dad1-HA and Ndc10-GFP fusion proteins were prepared for chromosome spreads as described (Loidl *et al.*, 1998; Cheeseman *et al.*, 2001). They were then processed for immunofluorescence and stained with anti-GFP antibodies to localize Ndc10-GFP and anti-HA antibodies to localize Dad1-HA. Bar, 2.5 μm.

Duo1p, Dam1p, and Dad1p Associate with Centromeric Loci In Vivo

In addition to localization to the mitotic spindle, we performed immunofluorescence on yeast chromosome spreads to determine whether Dad1p associates with chromatin. With the use of such an approach, Duo1p and Dam1p showed a punctate staining pattern that was coincident with the established kinetochore components Ndc10p and Mtw1p, but that only partially overlapped with Tub4p (Cheeseman *et al.*, 2001). On chromosome spreads, Dad1-HA also immunolocalized to punctate foci that exactly colocalized with the established kinetochore component Ndc10p (Figure 6), as well as Duo1p and Dam1p (our unpublished results). Therefore, in addition to localizing to the mitotic spindle, Dad1p also localizes with Duo1p and Dam1p to kinetochores.

Although Dad1p, Duo1p, and Dam1p colocalized with kinetochore structures and not to other places on the yeast chromosome, it was not clear whether these proteins associated specifically with the 125-bp yeast centromere. For this reason, we conducted chromatin immunoprecipitations (ChIP) on formaldehyde cross-linked yeast extracts (Meluh and Broach, 1999) with the use of affinity-purified anti-Duo1p and anti-Dam1p antibodies, and anti-myc antibodies with a Dad1-myc tagged strain. ChIP has been used previously to establish the centromere association of a number of candidate centromere proteins, including Mif2p, the yeast CENP-C homolog, and Ndc10p, a component of the essential CBF3 complex (Meluh and Koshland, 1997; Meluh *et al.*, 1998; Hyland *et al.*, 1999; Ortiz *et al.*, 1999). With the use of this approach, we found that Duo1p, Dam1p, and Dad1-myc all interact with centromeric DNA in vivo (Figure 7, A and B). In each case, the detected interaction was highly centromere-specific, as has been observed for other established centromere components (e.g., Mif2p or Ndc10p). Only *CEN*

DNA and sequences immediately flanking the centromere were enriched in the chromatin immunoprecipitates (Figure 7C). Other genomic loci (e.g., *LEU2*, *PGK1*) and centromere proximal regions were not enriched in the immunoprecipitates (Figure 7, A–C; our unpublished results), consistent with the localization pattern of these three proteins observed by indirect immunofluorescence microscopy (see above; Cheeseman *et al.*, 2001).

We next sought to determine how Duo1p and Dam1p interact with centromeric loci. We found that the interaction of Duo1p and Dam1p with *CEN* DNA was substantially diminished in an *ndc10-42* mutant upon shift to the restrictive temperature (Figure 7A). In fact, only 10–20% of centromeric association remains at 37°C in *ndc10-42* mutants based on a quantitation of the *CEN1* and *CEN3* signals (Table 2). This result indicates that the association of Duo1p and Dam1p with *CEN* DNA is largely dependent upon the integrity of the CBF3 complex, a prime determinant of centromere identity in budding yeast (McGrew *et al.*, 1986; Goh and Kilmartin, 1993; Sorger *et al.*, 1995; Meluh and Koshland, 1997; Ortiz *et al.*, 1999).

We also sought to determine whether the interaction of Duo1p, Dam1p, and Dad1p with centromeric DNA was dependent on microtubules (Figure 7D). Cells were first synchronized in G_1 with alpha factor and then released from alpha factor into fresh medium, or medium containing the microtubule-depolymerizing drug nocodazole. Interestingly, when ChIP was conducted on cells arrested in G_1, there was only 50–70% the amount of centromeric DNA associated with Duo1p, Dam1p, and Dad1-myc compared with cells released into fresh medium (Table 3). For these experiments, cells released into fresh medium showed a comparable level of centromeric DNA association to vegetatively growing cells (Figure 7, A and B; Table 2). Cells released into nocodazole showed a small additional decrease in the amount of centromeric DNA association compared with the alpha factor-arrested cells (25–50% of cells released to fresh medium; Table 3). A 50% reduction in centromeric association was also observed in cells shifted directly to medium containing nocodazole (our unpublished results). However, this reduction in centromere association is not as great as in the *ndc10* mutants that lack kinetochore function. In contrast, the association of core components, such as Mif2p and Cep3p (a component of the CBF3 complex), with centromeric DNA is unaffected by microtubule depolymerization.

In total, these results suggest that the kinetochore localization of the Duo1p/Dam1p/Dad1p complex is dependent on the presence of core kinetochore components, may be cell cycle regulated with lower amounts of centromere association during G_1, and that it is at least partially microtubule-dependent. Similar results have also been observed recently for the microtubule-associated protein Dis1 in *Schizosaccharomyces pombe* (Nakaseko *et al.*, 2001). It remains to be determined whether this indicates that Duo1p, Dam1p, and Dad1p are initially targeted to the kinetochore by microtubules, or whether a kinetochore-microtubule connection is required to maintain this localization.

We conclude that Duo1p/Dam1p/Dad1p protein complexes associate with yeast kinetochores in vivo. Based on their essential nature and on the direct microtubule binding activity of Dam1p (Hofmann *et al.*, 1998), we suggest Duo1p, Dam1p, and Dad1p might contribute to some aspect of the microtubule binding activity of the kinetochore.

DISCUSSION

Dad1p Is a Component of the Duo1p/Dam1p Complex

Here we have presented evidence that Dad1p is a novel third component of the Duo1p/Dam1p complex involved in spindle integrity and kinetochore function. Dad1p interacts physically with Duo1p by two-hybrid analysis, and it coimmunoprecipitates from yeast protein extracts with both Duo1p and Dam1p. This latter observation provides evidence that a Dad1p/Duo1p/Dam1p complex exists in vivo. Similar to Duo1p and Dam1p, Dad1p also localizes to both nuclear microtubules and kinetochores. Moreover, the localization of Dad1p to microtubules is dependent upon Duo1p and Dam1p. Several lines of genetic evidence provide further support to the conclusion that Dad1p functions as a component of the Duo1p/Dam1p complex. *DAD1* overexpression is able to partially suppress the phenotype, resulting from co-overexpression of *DUO1* and *DAM1*. *dad1-1* also shows genetic interactions with all alleles of *duo1* and *dam1*. Thus, mutations in *DAD1*, *DUO1*, or *DAM1* cause cells to be specifically sensitive to mutations in either of the other two genes. In addition, *dad1-1* shows a similar mitotic arrest phenotype to *duo1-2* and *dam1-9* mutants, indicating that *dad1* mutants are defective in a similar cellular process. Finally, similar to Duo1p and Dam1p, Dad1p is conserved in diverse fungal species. This observation suggests that the Duo1/Dam1/Dad1 complex plays an evolutionarily conserved role in spindle and kinetochore function. It remains to be determined whether there are more divergent homologs, or functional homologs, of these proteins in metazoan organisms.

Dad1p Is Required for Spindle Function and Chromosome Segregation

We demonstrated that *DAD1* is an essential gene in budding yeast. To determine the functions of Dad1p in vivo, we constructed a temperature-sensitive allele, *dad1-1*. Because *dad1-1* mutants activate the spindle assembly checkpoint, we conclude that these mutants have a spindle defect that is detected by this checkpoint. In fact, *dad1-1* single mutants and *dad1-1 duo1-1* double mutants showed broken down and bent spindles. Therefore, similar to a role that has been described for Duo1p and Dam1p, Dad1p is required for spindle integrity.

In addition to a role in spindle integrity, we have implicated Dad1p in chromosome segregation, possibly with a direct role in kinetochore function. Approximately 30% of *dad1-1* mutants undergo chromosome mis-segregation at the restrictive temperature as monitored with the use of the LacI-GFP system of chromosome tagging. Although this frequency of chromosome mis-segregation is not as high as was observed for some alleles of *dam1*, which show 90% mis-segregation at the restrictive temperature, it is similar to the frequency of mis-segregation observed for *duo1-2* and *dam1-9* mutants, which also arrest with a short mitotic spindle (Cheeseman *et al.*, 2001).

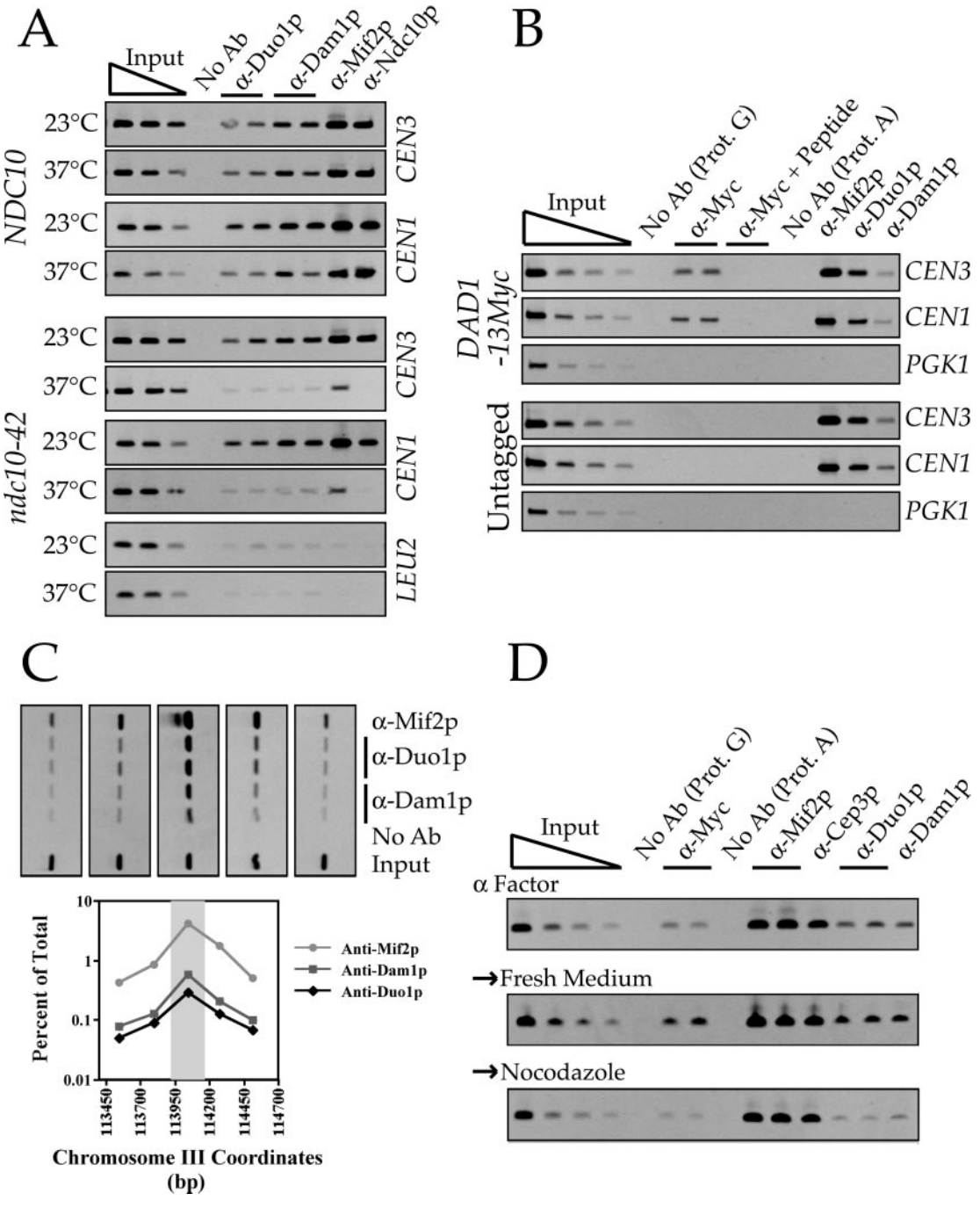

Figure 7. Duo1p, Dam1p, and Dad1p are present at centromeric loci in vivo. (A) Coimmunoprecipitation of *CEN* DNA with Duo1p and Dam1p. Wild-type (YPH499) and *ndc10-42* mutant (PM1021-20A) strains were grown at 23°C in YPD until mid-logarithmic phase (OD_{600} of ~0.5), at which point a portion of each culture was transferred to 37°C for 3 h. Formaldehyde cross-linked chromatin prepared from each culture was mock-treated (no antibody) or immunoprecipitated with the indicated antisera. Aliquots of total input material (~1.0, 0.5, and 0.25 μl of chromatin solution) and coimmunoprecipitated DNA (~100 μl of chromatin solution for Duo1p and Dam1p or ~50 μl for Mif2p and Ndc10p) were analyzed by PCR with primers specific for the indicated loci. Yields as a percentage of total input material are indicated in Table 2. Interaction of Duo1p and Dam1p with *CEN* DNA is centromere-specific and *NDC10*-dependent. (B) Coimmunoprecipitation of *CEN* DNA with Dad1-13myc. Dad1-13myc (DDY2166) and untagged strains (YPH499) were used for chromatin immunoprecipitation as in A, except an FA lysis buffer was used. To determine the specificity of this immunoprecipitation, myc peptide was in 200 or 500 M excess to myc antibody. (C) Interactions of Duo1p and Dam1p are limited to the *CEN* DNA. Total input material (~0.5 μl of chromatin solution) and coimmunoprecipitated DNA (~100 μl of chromatin solution for Duo1p and Dam1p or ~50 μl for Mif2p) from YPH499 were analyzed by PCR with the use of primers specific for a series of overlapping *CEN3*-flanking fragments. Below, the percentage of total input material that

Table 2. Quantitation of centromere association: Ndc10 dependence

		α-Duo1p	α-Dam1p	α-Mif2p	α-Ndc10p
NDC10	23°C	0.15	0.32	3.55	1.85
		0.16	0.28	1.98	1.20
	37°C	0.24	0.48	4.44	3.19
		0.15	0.28	1.74	1.71
ndc10-42	23°C	0.19	0.32	2.78	1.54
		0.12	0.22	1.99	0.65
	37°C	0.04	0.05	0.53	0.00
		0.03	0.04	0.21	0.00

The values correspond to the percentage of total centromeric DNA that is immunoprecipitated with the indicated antibody. The data in the top row of each section is for *CEN3*, whereas the data in bottom row is for *CEN1*. Each value is the average of duplicate immunoprecipitation reactions.

Table 3. Quantitation of centromere association: nocodazole treatment

	α-Duo1p	α-Dam1p	α-Myc	α-Mif2p
Alpha factor	1.20	1.48	0.92	7.4
⇒ Fresh medium	1.82	2.14	1.61	9.66
	2.15	2.45	1.51	12.78
⇒ Nocodazole	0.62	0.85	0.62	11.55
	0.72	0.99	0.65	18.28

The values correspond to the percentage of total centromeric DNA that is immunoprecipitated with the indicated antibody. The data in the top row of each section is for *CEN3*, whereas the data in the bottom row is for *CEN1*; Alpha factor data shown are for *CEN3*. Values are shown the averages of duplicate samples from both the tagged and untagged strains.

The role that Dad1p plays in chromosome segregation could be direct because we also found that Dad1p localized to kinetochores in spreads of mitotic chromosomes and associates with centromeric DNA by chromatin immunoprecipitation. We have also extended our previous studies on the kinetochore localization of Duo1p and Dam1p to demonstrate that these three proteins specifically associate with centromeric DNA by chromatin immunoprecipitation. In addition, we show that this association is largely dependent on Ndc10 function, indicating that kinetochore association of the Duo1p/Dam1p/Dad1p complex requires the presence of a core kinetochore structure. This centromere association is also partially dependent upon the presence of microtubules, and may be regulated over the course of the cell cycle with less association during G_1.

A Complex Connecting Spindle and Kinetochore Function

For chromosome segregation to occur, spindle microtubules must attach to each pair of sister chromatids. Despite the discovery of numerous kinetochore components and microtubule-associated proteins, the mechanism by which this connection is made remains to be elucidated fully. Given their dual association with both spindle microtubules and kinetochores, Duo1p, Dam1p, and Dad1p have the potential to connect kinetochores to the spindle. In addition, *duo1*, *dam1*, and *dad1* mutants each show high rates of chromosome mis-segregation and an apparent monopolar attachment of sister chromatids (this work; Cheeseman *et al.*, 2001), consistent with a role in mediating kinetochore–microtubule attachments.

To fully understand what role these proteins play in kinetochore–microtubule attachments, it will be necessary to identify all of the interactions made by Duo1p, Dam1p, and Dad1p. The link between Duo1p/Dam1p and Dad1p established here adds to previous work and indicates that these proteins form a ternary complex. It remains to be determined whether there are additional subunits of the Duo1p/Dam1p/Dad1p complex. Both Dad1p and Dam1p were identified in a two-hybrid screen with Duo1p (Hofmann *et al.*, 1998). This screen also identified other candidate genes that might interact with this complex. However, transcription of these genes is not regulated in a similar pattern to *DUO1*, *DAM1*, or *DAD1* (Spellman *et al.*, 1998), suggesting that they may not be integral components of the complex, or may have been false positives.

A recent genome-wide two-hybrid analysis has also indicated that both Duo1p and Dad1p interact with an additional spindle component, Spc34p (Ito *et al.*, 2000). Spc34p also interacts with the spindle component Spc19p. Both proteins were identified by mass spectrometry of proteins associated with purified spindle poles, and both localize along the entire length of mitotic spindles (Wigge *et al.*, 1998). Therefore, Spc34p and Spc19p have the potential to interact with Duo1p, Dam1p, and Dad1p in vivo and may function together with the Duo1p/Dam1p/Dad1p complex to facilitate aspects of spindle integrity or kinetochore function.

Finally, Duo1p and Dam1p have also been shown to interact physically with Sli15p and Ipl1p (Kang, Chan, and Cheeseman, unpublished data), which play a role in kinetochore function (Biggins *et al.*, 1999; Kim *et al.*, 1999). This web of interactions therefore provides an important link with other factors involved in both spindle and kinetochore

Figure 7 (cont). coimmunoprecipitated with each protein is plotted against the center coordinate for each interval amplified. The gray bar indicates the interval that encompasses *CEN3*. As for Mif2p (and for most centromere components), the interaction of Duo1p and Dam1p with the *CEN3* region occurs predominately at *CEN3*, whereas *CEN3*-flanking regions are enriched to a lesser extent. Identical results were also obtained for Dad1-13myc (our unpublished results). (D) Interaction of Duo1p, Dam1p, and Dad1-myc is partially dependent on microtubules. Dad1-13myc (DDY2166) and untagged (YPH499) strains were arrested in G_1 with 5 μM alpha factor for 2 h at 30°C (α factor). Portions of these cells were then washed two times and released into fresh medium (⇒ fresh medium), or medium containing 15 μg/ml nocodazole (⇒ nocodazole) for 1.5 h at 30°C. Microtubule depolyermization was confirmed by indirect immunofluorescence with an anti-β-tubulin antibody. All samples were then processed for chromatin immunoprecipitation as in A, although the FA lysis buffer was used for the Dad1-tagged strain. The data shown corresponds to *CEN3* for the Dad1-tagged strain. Yields of both *CEN3* and *CEN1* as a percentage of total input material were averaged for the tagged and untagged strains and are indicated in Table 3.

function. It will now be important to determine the stoichiometry of subunits in the Duo1p/Dam1p/Dad1p complex, to elucidate the specific functions of each individual subunit and the complex as a whole, and to determine how the functions of the complex are regulated.

ACKNOWLEDGMENTS

We thank Keith Kozminski for discussions and critical reading of the manuscript; and Ching Shang, Jonathan Wong, Christine Brew, and Tim Huffaker for discussions and advice. We also thank Shelly Jones, Mark Winey, and Sue Biggins for reagents, helpful discussions, and advice; and Kenneth Kaplan for the anti-Ndc10 antibody. This work was supported by a grant to G.B. from the National Institute of General Medical Sciences (GM-47842), a grant to P.B.M. from the National Institute of General Medical Sciences (RO1 GM-60464-02) and support of the Rosanne H. Silbermann Foundation, and a National Science Foundation Graduate Research Fellowship to I.M.C.

REFERENCES

Ayscough, K.R., and Drubin, D.G. (1998). Immunofluorescence microscopy of yeast cells. In: Cell Biology: A Laboratory Handbook, vol. 2, ed. J. Celis, New York: Academic Press, 477–485.

Belmont, A.S., and Straight, A.F. (1998). In vivo visualization of chromosomes using lac operator-repressor binding. Trends Cell Biol. *8*, 121–124.

Biggins, S., Severin, F.F., Bhalla, N., Sassoon, I., Hyman, A.A., and Murray, A.W. (1999). The conserved protein kinase Ipl1 regulates microtubule binding to kinetochores in budding yeast. Genes Dev. *13*, 532–544.

Cheeseman, I.M., Enquist-Newman, M., Müller-Reichert, T., Drubin, D.G., and Barnes, G. (2001). Mitotic spindle integrity and kinetochore function linked by the Duo1p/Dam1p complex. J. Cell Biol. *152*, 197–212.

Goh, P.-Y., and Kilmartin, J.V. (1993). NDC10: a gene involved in chromosome segregation in *Saccharomyces cerevisiae*. J. Cell Biol. *121*, 503–512.

Hofmann, C., Cheeseman, I.M., Goode, B.L., McDonald, K.L., Barnes, G., and Drubin, D.G. (1998). *Saccharomyces cerevisiae* Duo1p and Dam1p, novel proteins involved in mitotic spindle function. J. Cell Biol. *143*, 1029–1040.

Hyland, K.M., Kingsbury, J., Koshland, D., and Hieter, P. (1999). Ctf19p: a novel kinetochore protein in *Saccharomyces cerevisiae* and a potential link between the kinetochore and mitotic spindle. J. Cell Biol. *145*, 15–28.

Ito, T., Tashiro, K., Muta, S., Ozawa, R., Chiba, T., Nishizawa, M., Yamamoto, K., Kuhara, S., and Sakaki, Y. (2000). Toward a protein-protein interaction map of the budding yeast: a comprehensive system to examine two-hybrid interactions in all possible combinations between the yeast proteins. Proc. Natl. Acad. Sci. USA *97*, 1143–1147.

Jones, M.H., Bachant, J.B., Castillo, A.R., Giddings, T.H., and Winey, M. (1999). Yeast Dam1p is required to maintain spindle integrity during mitosis and interacts with the Mps1p kinase. Mol. Biol. Cell *10*, 2377–2391.

Kim, J.H., Kang, J.S., and Chan, C.S. (1999). Sli15 associates with the ipl1 protein kinase to promote proper chromosome segregation in *Saccharomyces cerevisiae*. J. Cell Biol. *145*, 1381–1394.

Kingsbury, J., and Koshland, D. (1993). Centromere function on minichromosomes isolated from budding yeast. Mol. Biol. Cell *4*, 859–870.

Loidl, J., Klein, F., and Engebrecht, J. (1998). Genetic and morphological approaches for the analysis of meiotic chromosomes in yeast. Methods Cell Biol. *53*, 257–285.

Longtine, M.S., McKenzie, A., Demarini, D.J., Shah, N.G., Wach, A., Brachat, A., Philippsen, P., and Pringle, J.R. (1998). Additional modules for versatile and economical PCR-based gene deletion and modification in *Saccharomyces cerevisiae*. Yeast. *14*, 953–961.

McGrew, J., Diehl, B., and Fitzgerald-Hayes, M. (1986). Single base-pair mutations in centromere element III cause aberrant chromosome segregation in *Saccharomyces cerevisiae*. Mol. Cell. Biol. *6*, 530–538.

Meluh, P.B., and Broach, J.R. (1999). Immunological analysis of yeast chromatin. Methods Enzymol. *304*, 414–430.

Meluh, P.B., and Koshland, D. (1997). Budding yeast centromere composition and assembly as revealed by in vivo cross-linking. Genes Dev. *11*, 3401–3412.

Meluh, P.B., Yang, P., Glowczewski, L., Koshland, D., and Smith, M.M. (1998). Cse4p is a component of the core centromere of *Saccharomyces cerevisiae*. Cell *94*, 607–613.

Nakaseko, Y., Goshima, G., Morishita, J., and Yanagida, M. (2001). M phase-specific kinetochore proteins in fission yeast: microtubule-associating Dis1 and Mtc1 display rapid separation and segregation during anaphase. Curr. Biol. *11*, 537–549.

Ortiz, J., Stemmann, O., Rank, S., and Lechner, J. (1999). A putative protein complex consisting of Ctf19, Mcm21, and Okp1 represents a missing link in the budding yeast kinetochore. Genes Dev. *13*, 1140–1155.

Pasqualone, D., and Huffaker, T.C. (1994). STU1, a suppressor of a beta-tubulin mutation, encodes a novel and essential component of the yeast mitotic spindle. J. Cell Biol. *127*, 1973–1984.

Pellman, D., Bagget, M., Tu, Y.H., Fink, G.R., and Tu, H. (1995). Two microtubule-associated proteins required for anaphase spindle movement in *Saccharomyces cerevisiae* [published erratum appears in J. Cell Biol. (1995) *131*, 561]. J. Cell Biol. *130*, 1373–1385.

Pidoux, A.L., and Allshire, R.C. (2000). Centromeres: getting a grip of chromosomes. Curr. Opin. Cell Biol. *12*, 308–319.

Roof, D.M., Meluh, P.B., and Rose, M.D. (1992). Kinesin-related proteins required for assembly of the mitotic spindle. J. Cell Biol. *118*, 95–108.

Rose, M.D., Winston, F., and Hieter, P. (1990). Methods in Yeast Genetics, Cold Spring Harbor, NY: Cold Spring Harbor Laboratory Press.

Saunders, W., Lengyel, V., and Hoyt, M.A. (1997). Mitotic spindle function in *Saccharomyces cerevisiae* requires a balance between different types of kinesin-related motors. Mol. Biol. Cell. *8*, 1025–1033.

Saunders, W.S., and Hoyt, M.A. (1992). Kinesin-related proteins required for structural integrity of the mitotic spindle. Cell *70*, 451–458.

Severin, F.F., Sorger, P.K., and Hyman, A.A. (1997). Kinetochores distinguish GTP from GDP forms of the microtubule lattice. Nature *388*, 888–891.

Sorger, P.K., Doheny, K.F., Hieter, P., Kopski, K.M., Huffaker, T.C., and Hyman, A.A. (1995). Two genes required for the binding of an essential *Saccharomyces cerevisiae* kinetochore complex to DNA. Proc. Natl. Acad. Sci. USA *92*, 12026–12030.

Sorger, P.K., Severin, F.F., and Hyman, A.A. (1994). Factors required for the binding of reassembled yeast kinetochores to microtubules in vitro. J. Cell Biol. *127*, 995–1008.

Spellman, P.T., Sherlock, G., Zhang, M.Q., Iyer, V.R., Anders, K., Eisen, M.B., Brown, P.O., Botstein, D., and Futcher, B. (1998). Com-

prehensive identification of cell cycle-regulated genes of the yeast *Saccharomyces cerevisiae* by microarray hybridization. Mol. Biol. Cell *9*, 3273–3297.

Straight, A.F., Sedat, J.W., and Murray, A.W. (1998). Time-lapse microscopy reveals unique roles for kinesins during anaphase in budding yeast. J. Cell Biol. *143*, 687–694.

Uetz, P., L. Giot, G. Cagney, T.A. Mansfield, R.S. Judson, J.R. Knight, D. Lockshon, V. Narayan, M. Srinivasan, P. Pochart, A. Qureshi-Emili, Y. Li, B. Godwin, D. Conover, T. Kalbfleisch, G. Vijayadamodar, M. Yang, M. Johnston, S. Fields, and J.M. Rothberg. (2000). A comprehensive analysis of protein-protein interactions in *Saccharomyces cerevisiae* [see comments]. Nature *403*, 623–627.

Wigge, P.A., Jensen, O.N., Holmes, S., Soues, S., Mann, M., and Kilmartin, J.V. (1998). Analysis of the *Saccharomyces* spindle pole by matrix-assisted laser desorption/ionization (MALDI) mass spectrometry. J. Cell Biol. *141*, 967–977.

Winey, M., Mamay, C.L., O'Toole, E.T., Mastronarde, D.N., Giddings, T.H., McDonald, K.L., and McIntosh, J.R. (1995). Three-dimensional ultrastructural analysis of the *Saccharomyces cerevisiae* mitotic spindle. J. Cell Biol. *129*, 1601–1615.

Winey, M., and O'Toole, E.T. (2001). The spindle cycle in budding yeast. Nat. Cell Biol. *3*, E23–E27.

Winsor, B., and Schiebel, E. (1997). Review: an overview of the *Saccharomyces cerevisiae* microtubule and microfilament cytoskeleton. Yeast *13*, 399–434.